Smart Structures and Systems, *Vol. 13, No. 6 (2014) 993-1014*
DOI: http://dx.doi.org/10.12989/sss.2014.13.6.993

Development of a dynamic sensing system for civil revolving structures and its field tests in a large revolving auditorium

Yaozhi Luo[1a], Pengcheng Yang[1b], Yanbin Shen[*1], Feng Yu[1], Zhouneng Zhong[2] and Jiangbo Hong[3]

[1]*Department of Civil Engineering, College of Civil Engineering and Architecture, Zhejiang University, Hangzhou, Zhejiang Province, 310058, P. R. China*
[2]*Zhejiang Greenton Architectural Design Co., Ltd, Hangzhou 310007, P. R. China*
[3]*Hanjia Design Group Co., Ltd, Hangzhou 310005, P. R. China*

(Received November 11, 2013, Revised March 25, 2014, Accepted March 30, 2014)

Abstract. In civil engineering, revolving structures (RS) are a unique structural form applied in innovative architecture design. Such structures are able to revolve around themselves or along a certain track. However, few studies are dedicated to safety design or health monitoring of RS. In this paper, a wireless dynamic sensing system is developed for RS, and field tests toward a large revolving auditorium are conducted accordingly. At first, a wheel-rail problem is proposed: The internal force redistributes in RS, which is due to wheel-rail irregularity. Then the development of the sensing system for RS is presented. It includes system architecture, network organization, vibrating wire sensor (VWS) nodes and online remote control. To keep the sensor network identifiable during revolving, the addresses of sensor nodes are reassigned dynamically when RS position changes. At last, the system is mounted on a huge outdoor revolving auditorium. Considering the influence of the proposed problem, the RS of the auditorium has been designed conservatively. Two field tests are conducted via the sensing system. In the first test, 2000 people are invited to act as the live load. During the revolving process, data is collected from RS in three different load cases. The other test is the online monitoring for the auditorium during the official performances. In the end, the field-testing result verifies the existence of the wheel-rail problem. The result also indicates the dynamic sensing system is applicable and durable even while RS is rotating.

Keywords: revolving structure; sensing system; field test; dynamic addressing; wheel-rail; structural health monitoring; system development

1. Introduction

In contemporary architecture, kinetic structures have freed designers from traditional ideas of structural form. Instead of standing still on the ground permanently, part or whole of kinetic buildings can transform or move (Ramzy and Fayed 2011).The use of robotics, mechanics and electronics is essential to carry out this new idea. Revolving structure (RS) is one kind of dynamic

∗Corresponding author, Assistant Professor, E-mail: benjamin127@163.com
[a] Professor, E-mail: luoyz@zju.edu.cn
[b] Ph. D. Student, E-mail: imyouth@163.com

http://www.techno-press.org/?journal=sss&subpage=8 ISSN: 1738-1584 (Print), 1738-1991 (Online)

kinetic structures and can revolve around itself or along a certain track. RS allows varying views and alters the orientation for different needs of architects. Its development started early since 1906, throughout the 20th century, and continued to this day (Randl 2008). Some designs are timeless classics, such as Villa Girasole in Verona, Italy, built in 1935, a 25 m-by-25 m L-shaped wooden house, rotating on 15 sets of wheels (Frampton *et al*. 2006), Heliotrope House in Freiburg, Germany, built in 1994, a 10.5 m-diameter tower-type revolving tree house (Wigginton and Harris 2002), and so on. To a certain extent, RS is similar to a super gigantic train carrying passengers on tracks, and it needs wheels and rails. Studies on railway vehicle/track interaction have been carried on since the last century (Timoshenko 1926, Sato 1977, Grassie *et al*. 1982, Thompson 1991, Knothe and Grassie 1993). Vehicles are affected by wheel-rail interaction forces and track irregularities. Besides, for large RS, the weight is a lot heavier, and the scale of wheel-rail relations is much greater. It has a significant influence on the safety of RS.

However, there is little discussion concerned with the wheel-rail influence among those previous studies of RS. To confirm the influence, it is necessary to build a suitable structural health monitoring (SHM) system for RS and conduct field tests on a specific revolving building. When considering SHM system for RS, wireless sensor network (WSN) technique is more helpful, because it avoids vast wiring workload and high-maintenance cost of traditional wired SHM. Furthermore, when sensors are installed on the movable parts of structures, layout problem of signal wires will not be a concern. In the field of SHM based on WSN, many researchers have developed their own sensor nodes (Spencer *et al*. 2004) or sensing systems. There are classic works (Straser and Kiremidjian 1998, Lynch *et al*. 2004, Wang *et al*. 2005, Sazonov *et al*. 2006, Wang *et al*. 2007, Nagayama *et al*. 2009) and some recent works (Zhu *et al*. 2010, Myung *et al*. 2011, Wang and Law 2011, Kim *et al*. 2013, Yun *et al*. 2013). They are aimed at improving the accuracy and system stability, reducing energy consumption of sensor nodes, and increasing success rate of damage identification. There is no lack of classic practical applications of WSN in civil engineering, including SHM of long-span bridges(Lynch *et al*. 2006, Kim *et al*. 2007), high-rise buildings (Ni *et al*. 2009), large-span spatial structures(Teng *et al*. 2010), etc.

Preceding studies about SHM of WSN mainly focus on conventional motion less structures. Only a few SHM studies of movable bridges have been carried out(Catbas *et al*. 2010, Dumlupinar *et al*. 2011, Gokce *et al*. 2012).However, the movability of those bridges is rather limited, and therefore, their monitoring tools are implemented with wired sensing systems. There is barely SHM work with WSN systems aiming for dynamic kinetic structures, not to mention for RS. For RS monitoring system, considering the special features of RS, some new problems are expected to arise concerning networking of sensor nodes in a rotating field, sensor durability, sensing feedback for revolving control, etc.

The principal purpose of this paper is to find out the wheel-rail impact on RS and monitor the behaviors of RS. The core approach is to develop and install a permanent sensing system on RS. The ultimate task is to plan and conduct experiments on real RS buildings. In the first half of the paper, the problem of wheel-rail influence on RS is proposed, and then the development of the sensing system is introduced in details, including dynamic networking method, remote control and so on. In the second half of the paper, two field-testing experiments are carried out on a large outdoor revolving auditorium, including a 2000-people test run and an online monitoring for commercial performance. Finally, data is collected, and the conclusions are achieved according to the results.

2. Smart RS in civil engineering

2.1 The mechanism

RS usually consists of a stiff structure as a rotator and one or more fixed circular tracks. As shown in Fig. 1, the rotator, with a certain number of wheels on it, can carry the load (including both dead load and live load) and revolve around a center axis. A tractive force or an equivalent torque, namely T_m, is applied on the rotator by some actuators that are usually powered by hydraulic pressure or electric energy. Thus, along the tracks, the rotator can be controlled to rotate to any wanted angle θ.

In Fig. 1, when RS is in a state of rest, its static structural behavior is determined by a finite-element formula

$$(\mathbf{K}_S + \mathbf{K}_C)\mathbf{X} = \mathbf{F}^{ext} \tag{1}$$

where $\mathbf{K}_S$ is the stiffness matrix of the rotator structure without any boundary condition modification, $\mathbf{K}_C$ is the support stiffness matrix, $\mathbf{F}^{ext}$ is the external force vector of load and $\mathbf{X}$ is the node displacement vector of RS. $\mathbf{K}_C$ is a function of the wheel, rail and foundation stiffness vectors, $\mathbf{k}_W$, $\mathbf{k}_R$ and $\mathbf{k}_F$. Considering construction error, $\mathbf{k}_R$ and $\mathbf{k}_F$ are related to the RS position of angle, θ, so Eq. (1) is rewritten as

$$\left[\mathbf{K}_S + f\left(\mathbf{k}_W, \mathbf{k}_R^{\theta}, \mathbf{k}_F^{\theta}\right)\right]\mathbf{X} = \mathbf{F}^{ext} \tag{2}$$

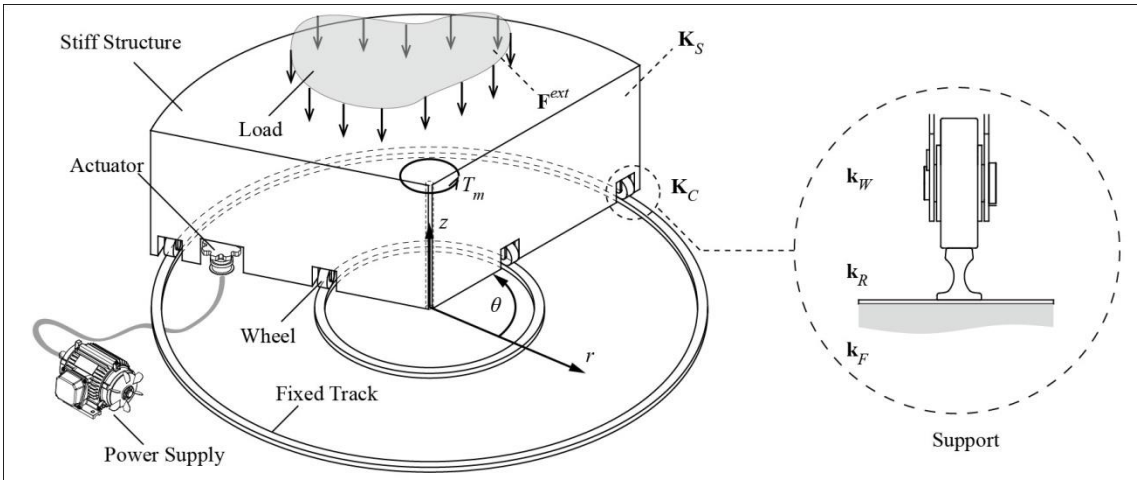

Fig. 1 Revolving structure (RS) in civil engineering

2.2The characteristics: Wheel-rail influence

The uses of RS determine the structure is by no means a motionless building, and its mechanical state changes when it revolves. It affects contact conditions and interactions between wheels and rails. Taking studies on railway vehicle/track interaction and irregularity for

reference(Timoshenko 1926, Sato 1977, Grassie *et al.* 1982, Thompson 1991, Knothe and Grassie 1993, Barke and Chiu 2005, Steffens 2005), we suppose RS has a similar problem. As Fig. 2 shows, wheel-rail contact cannot be ideally smooth and tight because of rail manufacturing error, foundation subsidence, butt welded joint, pollution and erosion of rainwater and dust, wheel manufacturing error or wearing out over time, etc. Further, when RS has many wheels, the situation is more complex. Under all those wheels, top surfaces of rails are most likely not in one same plane. Then some wheels detach from rails, and their reaction forces from the foundation, f_R, are equal to zero, so RS loses vertical support at positions of those wheels.

Such wheel-rail irregularity causes RS internal force redistribution when its position changes. For example, in the position of the angle θ, the internal force result based on the solution of Eq. (2) is indicated as the node stress matrix, $\mathbf{\Sigma}_\theta$. Therefore, after RS has rotated to the angle θ', the result becomes $\mathbf{\Sigma}_{\theta'}$.

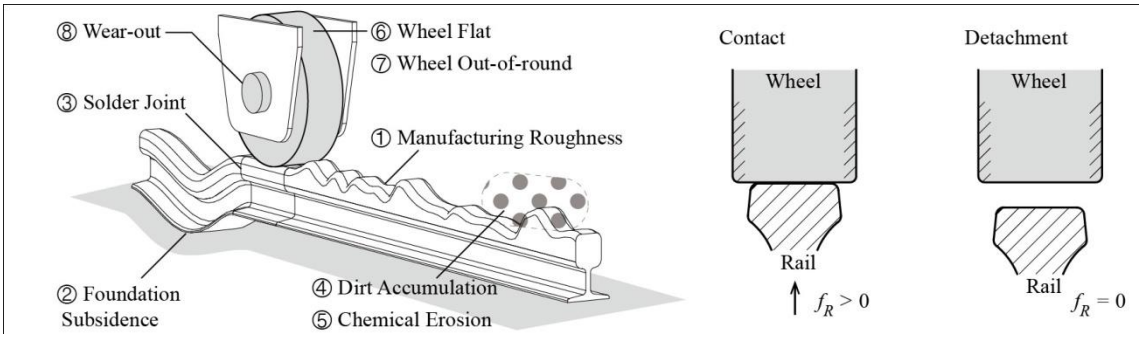

Fig. 2 Wheel-rail problem

2.3 Sensing system for reliability of RS

RS is like a train carrying passengers on tracks. When it rotates, it will suffer wheel-rail irregularity; and therefore, its internal force values vary. For structural safety, variations of internal forces must not exceed the range of material strength, so priority should be given to collecting the internal force information in real time.

A sensing system installed on RS can be helpful in this case. It collects data during RS rotation and passes data to RS control system. It also can process data and transfer results to remote computers for further analysis. The following conditions should be met before the system can work normally:

●**Collecting internal force data.** Sensors installed on RS should be able to measure internal forces. There also should be devices converting the analogue signal and collecting data.

●**Remote control and online processing.** The system should be controllable for both onsite and remote operations. The data can be processed and shared through the Internet.

●**Robustness not affected by RS rotation.** When sensors or other devices rotate with RS, their absolute positions change. Under this circumstance, the system should keep stability of its internal data transmission. The communication between the system and outside terminals should not be affected by the position changing.

●**Easy installation and durability.** For outdoor use, installation cost should be as low as possible. Sensors and devices should have some corrosion-resisting and waterproof abilities during long-term operation.

3. Development of sensing system embedded in RS

3.1 System architecture design and field condition

Wireless sensor network (WSN) technique is an effective way to organize the sensing system. With the help of WSN, the system has obvious advantages compared to traditional wired systems. For example, installation cost can be much lower; the system is easier to maintain; impact on structures is smaller; and so on. For health monitoring of movable structures, WSN gives planners greater flexibility in the system arrangement.

Generally, in WSN, all sensor nodes scattered in the sensor field collect data and route data back to the sink node (Akyildiz *et al*. 2002), and the design of sensing system follows this principle. Fig. 3 shows basic framework of the system. Sensor nodes are fixed onto RS and organized into a tree-type network of Radio Frequency (RF). As the root of the entire network, the sink node transfers all data gathered from sensor nodes to target devices in both onsite and remote ways. In the former way, the sink node communicates straightly with onsite devices through USB or serial ports. In the latter way, the sink node accesses the mobile internet by General Packet Radio Service (GPRS) or Wideband Code Division Multiple Access (WCDMA), so that it communicates with online devices. Thus, the system can be controlled remotely for automated long-term monitoring.

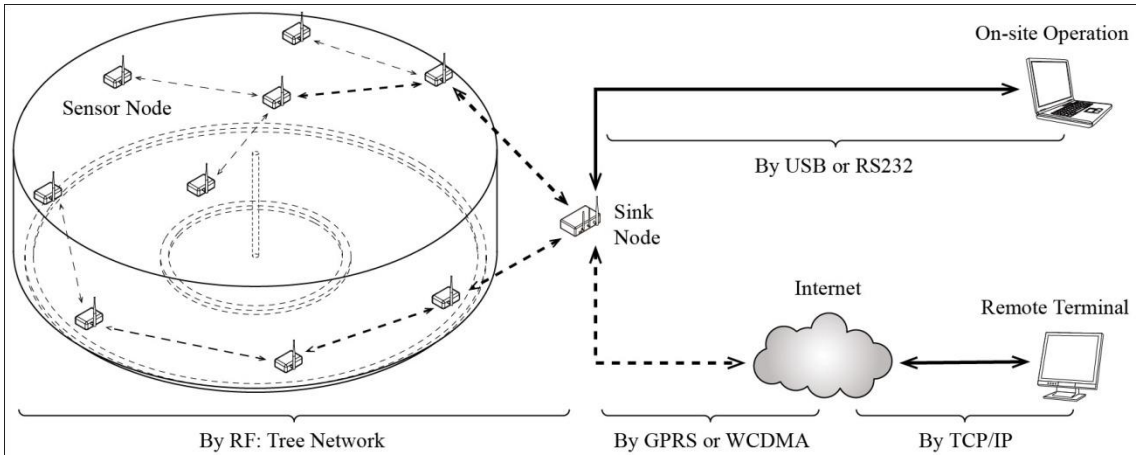

Fig. 3 Sensing system for RS: Overall scheme

Theoretically, the sink node and other devices used for the remote control can be fixed on the RS and rotate together. However, the condition is always complex in the field. On the movable

parts of civil structures, there is often no electricity to supply power, or there may not be proper places designed for that purpose. In some circumstances, the sink cannot rotate together with the structure, and it has to be placed somewhere away from the structure. In this paper, with the help of WSN, devices do not all have to rotate with RS, which brings great convenience to equipment arrangement. Low power sensors are battery-powered and have small sizes. They can be installed on RS, and rotate with it. Then the sink node and the other devices can be placed somewhere convenient.

3.2 Dynamic wireless network with custom protocol for revolving sensor fields

Once the position of the sink node is fixed somewhere away from RS, sensor nodes are configured to establish connections among themselves and route to the sink node. However, while all sensor nodes are rotating together with the RS, the relative position of sensor nodes to sink node will keep changing. After RS has rotated to a different position, the original network topology may not work because some data transmissions may disconnect due to the limit of communication distance.

To solve this problem, the studies of dynamic address assignment (Felegyhazi 2001, Basheer *et al.* 2003, Yao and Dressler 2007, Tomas and Gonzalo 2012) for WSN are used for reference. As Fig. shows, all sensors are organized as one or several subnets, and these subnets form a tree-type topology taking the sink node as the root. The number of subnets is determined by communication distances between nodes. If the communication radius, r_C, is larger than distance between the sink node and the center of RS, d_S, only one subnet can cover whole RS; otherwise, if $d_S > r_C$, one subnet is not enough. Considering transmission power limit and reception rate reduction by structures (Linderman *et al.* 2010), communication distance is rather limited. Meanwhile, in practical applications in civil engineering, RS can always be large. Therefore, there would be usually more than one subnet covering the entire structure.

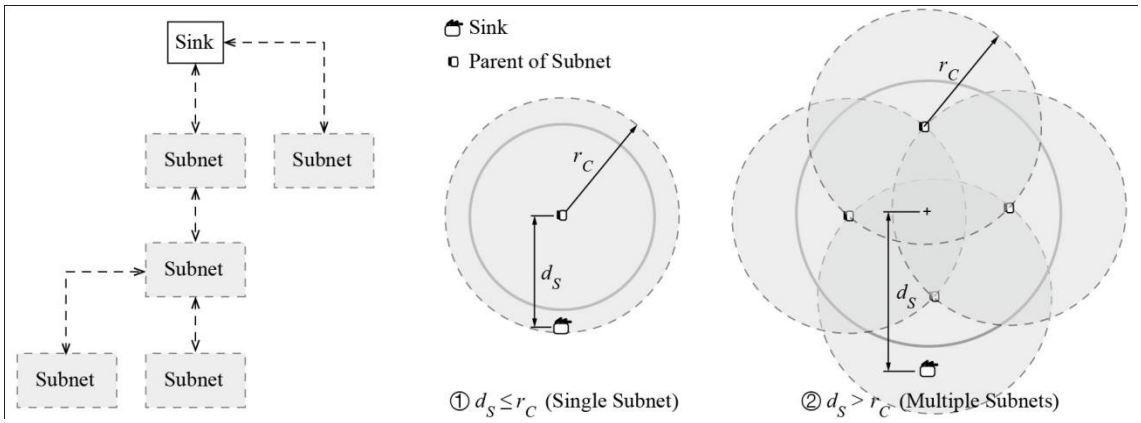

Fig. 4 Network coverage

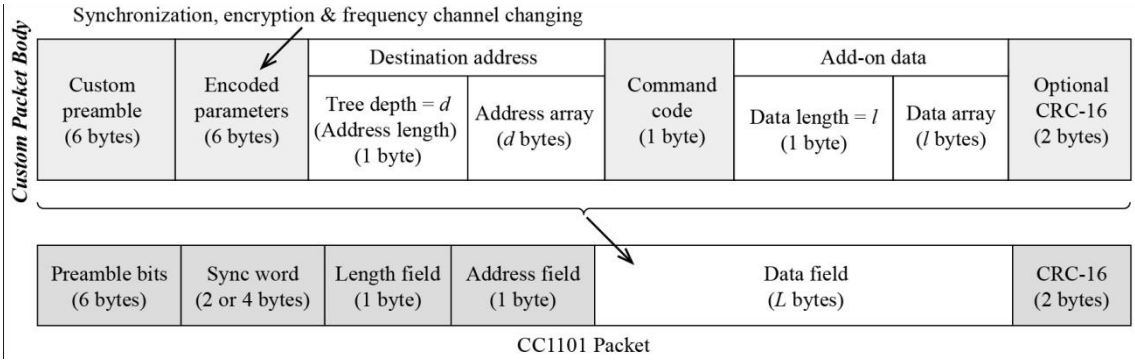

Fig. 5 Packet form

Considering the requirement of energy conservation and influence of certain obstacles, CC1101 transceiver of Texas Instruments is chosen for RF module of sensor nodes. It is a low-cost sub-1 GHz RF transceiver designed for low-power wireless applications. Based on CC1101 basic packet format, a custom packet formation is created, as fig. 5 shows. The custom packet is put into the data field of CC1101 packet. It contains address information, command type, data and some other parts about security.

For this tree network of one sink and multiple subnets, the main advantage is fast self-routing (Basheer *et al*. 2003). If the sensor nodes are assigned an address reflecting their distance from the sink node, then the packets could be routed within the network just according to the destination address in the packet. For instance, a sensor node is assigned an address

$$s = \left[b_1.b_2.b_3....b_d\right] \tag{3}$$

where b represents one address byte, and d is the tree depth of the sensor node in the network. Then a packet sends from the sink node, $[b_1]$, to this sensor node, s, will be routed as$[b_1]$ ->$[b_1.b_2]$ ->… -> $[b_1.b_2.\cdots.b_{d\text{-}1}]$ ->s, and vice versa. The total length of the custom packet

$$L_p = d + l + c \tag{4}$$

where l is the length of the add-on data, and c is a fixed constant. In Fig. 5, the constant c equals to 17. It can be seen that the custom protocol can make development progress more flexible and shorten the length of packets so that bandwidth cost is reduced.

After subnets have rotated together with RS to a new position, their connections to the sink node will be redefined by reassigning new addresses to some nodes. In other words, the tree topology of subnets will be reorganized to make communication of the entire network remain available. In each subnet, one parent node corresponds to several child nodes. When the node address of some subnets needs to be reassigned, its parent-child relation remains the same, and their global level in the tree network is changed as needed. For each subnet to reconfigure, only the common part of addresses will need to be modified. For instance in a subnet, there is a parent, $[\mathbf{B}_p]$, and n children,$[\mathbf{B}_p.b_{c,1}]$, $[\mathbf{B}_p.b_{c,2}]$, …, $[\mathbf{B}_p.b_{c,n}]$, where $\mathbf{B}_p$ is the address segment of the parent, and b_c represents one address byte of child nodes. After address reassigment, they become $[\mathbf{B'}_p]$, $[\mathbf{B'}_p.b_{c,1}]$, $[\mathbf{B'}_p.b_{c,2}]$, …, $[\mathbf{B'}_p.b_{c,n}]$.

For each node, there is a list of addresses corresponding to multiple sections of reassignment positions. For the address of a sensor node, s

$$\begin{aligned} &\text{let } s = s_1, s_2, \ldots \text{or } s_k, \\ &\text{when } \theta \in [\theta_1, \theta_2), [\theta_2, \theta_3), \ldots \text{or } [\theta_k, \theta_1). \end{aligned} \tag{5}$$

where k represents the quantity of possible position sections during RS 360-degree rotating. Once the RS position satisfies a certain condition in a section, the node address will be changed to the corresponding value; and accordingly, the network will be reorganized. Fig. 6 shows a simple example that how dynamic address assignment works. In the example, it can be seen that when $\theta = \theta_2$, the address of the parent node in Subnet 1 remains as [0.1] -> [0.1], and the node in Subnet 2 changes as [0.1.2] -> [0.2].

A simple simulation is performed to evaluate the performance of this approach for RS. In the simulation, the number of subnets, n_s, is determined as Fig. 4 shows, and the total number of nodes is assumed to be proportional to n_s. The whole RS area is assumed to be divided equally into subnets. Because RS usually revolves in ultra-low speed, the bandwidth is assumed to be always sufficient for low sample frequency. Besides, it is assumed that there is no packet loss for a static tree network. With a self-development program in MATLAB, the simulation is executed. As Fig. 7 shows, three metrics are considered to validate the effectiveness in terms of different n_s. The metrics include k mentioned before, Packet Delivery Ratio, r_p, and maximum value of End to End delay, $t_{d,\max}$. It can be seen that r_p always remains 100%, which means that address reassignment for RS matters very little to r_p.

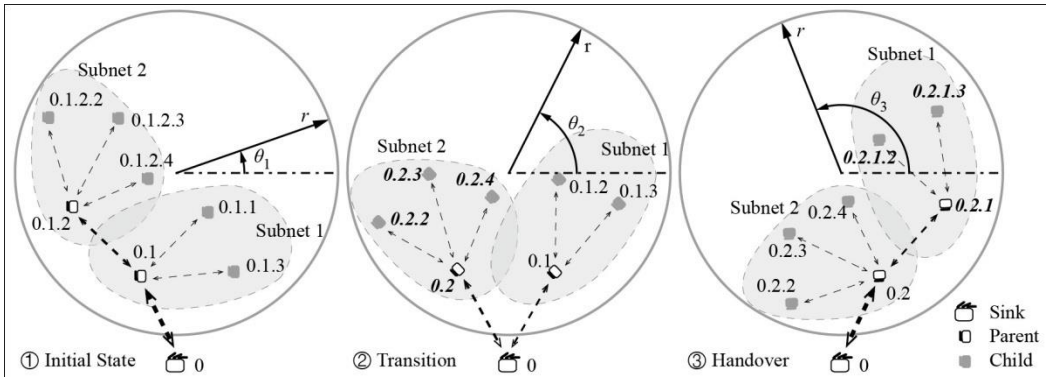

Fig. 6 Dynamic address assignment: Route changing

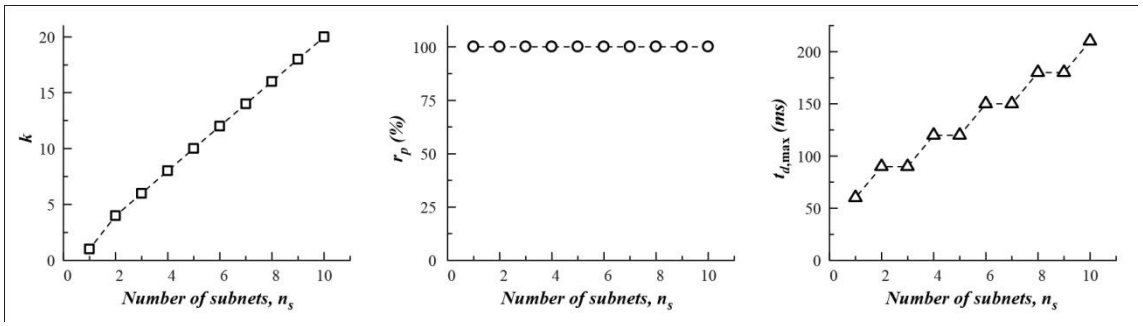

Fig. 7 Performance evaluation

3.3 Sensor nodes

3.3.1 Basic hardware

In general, hardware design of wireless sensor systems consists of four parts: data acquisition, digital wireless communication, embedded microprocessor and power management (Straser and Kiremidjian 1998, Lynch *et al.* 2003). Following a modular design idea, a basic hardware represented by a mainboard in this paper is integrated. Fig. 8 shows the structure and finished product of the mainboard. As shown in the block diagram of the figure, on the mainboard, there are several basic and necessary components including ① microcontroller, ② RF module (CC1101), ③ power management integrated circuit (IC) chips, ④ static random access memory (SRAM) and ⑤ interfaces for other boards. The sequence numbers of the photo in Fig. 8(b) correspond to the same as those of Fig. 8(a). As the photo shows, the mainboard is double-layered and rectangular.

3.3.2 Vibrating wire sensor node for internal force sensing

Among methods used to conduct strain measurements nowadays, three most prevalent ones are resistive strain gages (RSG), vibrating wire sensors (VWS) and fiber Bragg grating sensors (FBGS). To develop the sensing system in this paper, VWSs are considered more proper than the others. On one hand, VWSs are more durable than RSGs for outdoor long-term monitoring, and they are easier to install than RSGs. On the other hand, compared with FBGSs, VWSs cost less money and time for the development. They are cheaper than FBGSs, and the demodulation circuit of VWS signals is simpler so that the development cycle can be shortened. Besides, many studies and field applications of VWS shave proven this (Coutts *et al.* 2001, Bourquin and Joly 2005, Neild *et al.* 2005, Yu and Gupta 2005, Bourland and Yuan 2008).Major parts of a VWS consist of a vibrating wire whose frequency changes in response to tension and compression, and one plucking and pickup coil that excites the wire and reads its vibrating frequency (Lee *et al.* 2010). Since VWS products are now commercially available, only a corresponding expansion module is needed to consist of a VWS node. The details of the module are shown in Fig. 9, and the foremost function of the module is to process the signal of VWS.

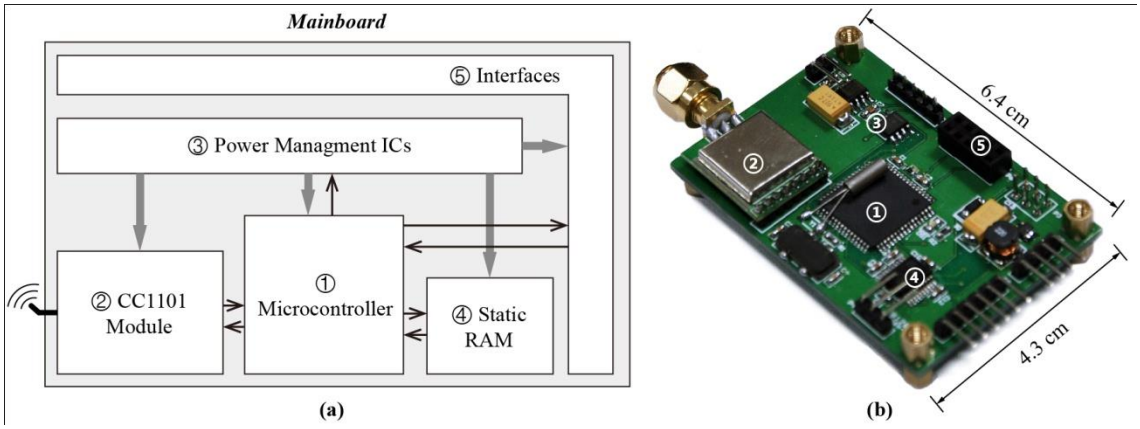

Fig. 8 Block diagram (a) and photograph (b) of the mainboard in sensor nodes

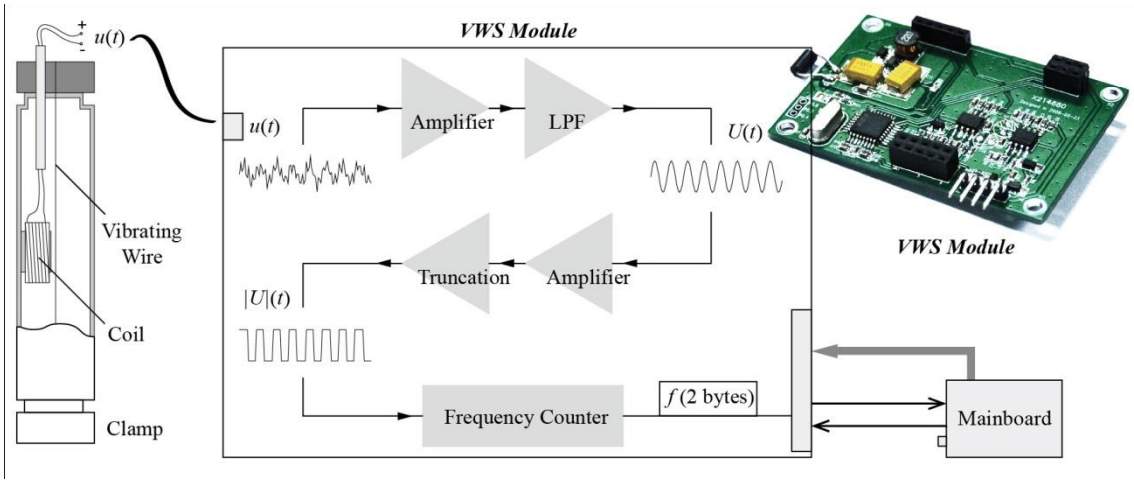

Fig. 9 Block diagram of vibrating wire sensor (VWS) node

As fig. 9 shows, an analogue voltage signal of VWS vibration, $u(t)$,is amplified and processed by low-pass filter (LPF), only leaving the first-order component, which can be expressed as

$$\beta u(t) = U(t) + u_H(t) = U_m \sin(2\pi f t) + u_H(t) \tag{6}$$

where $u(t)$ is amplified by a factor of β, $u_H(t)$ is higher-order components to be filtered out, $U(t)$ is the first-order component of the signal amplified, and U_m and f are amplitude and frequency of $U(t)$. With f, the VWS strain value εcan be exressed as

$$\varepsilon = f^2 L^2 \frac{4\rho}{Eg} \tag{1}$$

where L is the length of the vibrating wire,ρ is the density of the wire, E is Young's modulus, and g is gravitational acceleration. To get the frequency f, $U(t)$ is processed to be a square voltage signal of the same frequency, $|U|(t)$, as below

$$|U|(t) = \begin{cases} \text{High}, & n_N T \le t < (n_N + 0.5)T; \\ \text{Low}, & (n_N + 0.5)T \le t < (n_N + 1)T \end{cases} \cdot \left(T = 1/f, n_N \in N \right) \tag{8}$$

where T is the period of $U(t)$, and n_N belongs to the set of natural numbers. Then VWS module and the mainboard are grouped into a VWS node, and square wave $|U|(t)$ has been sent into the mainboard as a digital signal. With the digital input capture pins of the microcontroller, the value of f can be calculated, and the strain data is obtained accordingly. As stated previously, commercial VWS products are used, so the validation of the VWS node is evaluated in terms of frequency precision measured from VWS. In the waveform graph of Fig. 10(a), $u(t)$ is on CH2, and $|U|(t)$ on CH1 shows the effect of signal converting. Fig. 10(b) is the result of the compression and tension experiments. In the figure, a commercial VWS readout device is used to provide standard values of f. With the variation of ε from -2.0e-4 to 5.0e-4, $f$is measured from standard devices and VWS nodes. The maximum error of test values is about 1.2 Hz (0.08%) with respect to the standard values.

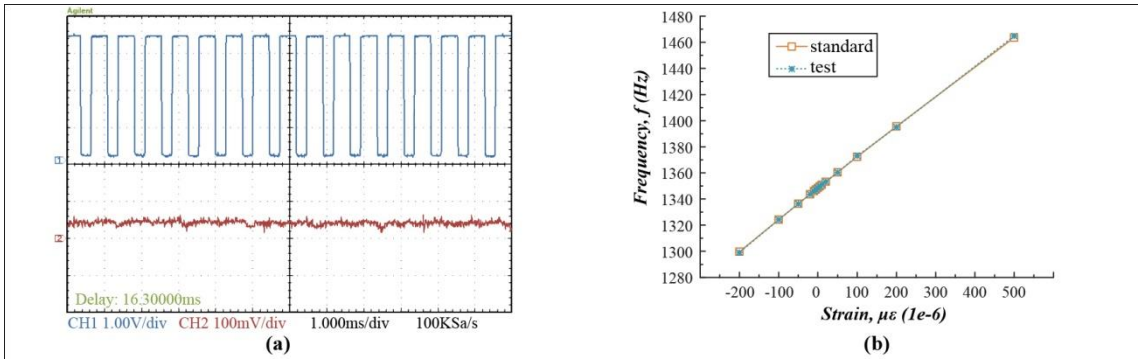

Fig. 10 Test results of VWS nodes: (a) Signal converting; (b) Comparison of strain in the compression and tension experimental test

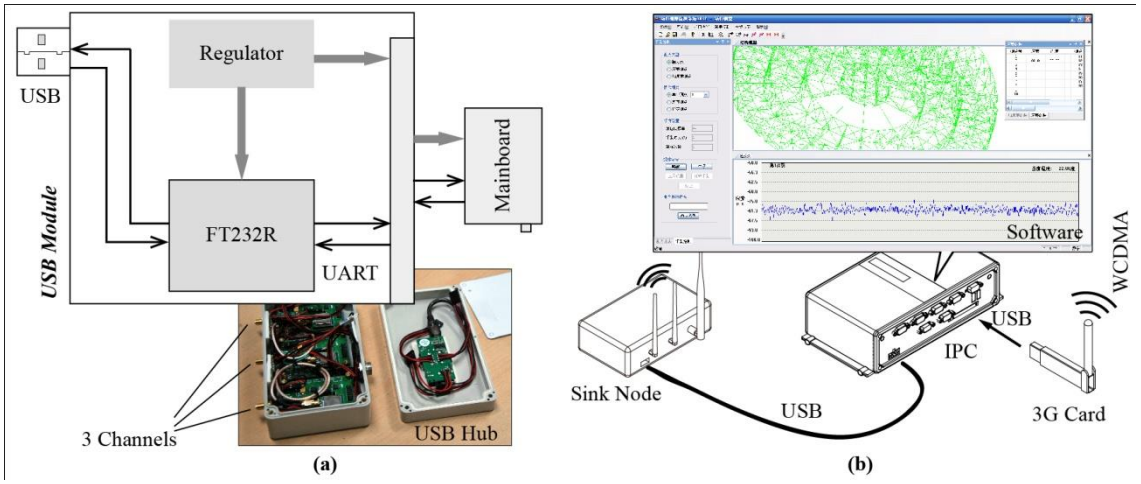

Fig. 11 (a) Sink node; (b) Remote control via the Internet

3.4 Remote control: hardware fabrication and software development

As previously stated in Section 3.1, data collected from sensor nodes to the sink node can be transmitted to the Internet. In the other way around, sensor nodes can receive action instruction from terminal devices through the Internet. The sink node is an important part of this remote procedure. Fig. 11(a) shows the structure of the sink node. The sink node consists of the mainboard and a special expansion board, similar to VWS nodes. For the communication between the sink node and a personal computer (PC),FT232R, a USB to serial UART interface of FTDI (Future Technology Devices International), is adopted. In the sensing system, a three-channel sink node is assembled. Fig. 11(b) shows that how the sink node connects to WCDMA mobile internet: Sink node connects with an industrial PC (IPC), and IPC accesses the Internet via a 3G card (network adapter of the third generation of mobile telecommunications technology).Thus, with various interfaces and access to the Internet, IPC can be controlled by other PCs in both onsite way

and remote way. In the sensing system, data transmission between the sensor field and terminals, data sharing and data processing are performed with the support of corresponding software. For example, in Fig. 11(b), software installed in the IPC provides functions of identifying sink node interface, collecting data from sensor nodes, controlling and configuring sensor network, planning and executing scheduled tasks, storing and uploading data to terminal devices via the Internet, etc.

4. RS field test

4.1 A large outdoor revolving auditorium: design and construction

An outdoor musical show *Impression Dahongpao*, directed by Chinese film director Zhang Yimou, is set on Wuyi Mountain in China. For this show, a large revolving auditorium is engineered to offer audiences a 360-degree view and use natural landscapes as both the stage and the background. Fig. 12 shows the structure design details. Having a structure of a steel truss skeleton, a diameter of 46.6 meters and a weight of 520 tons, the auditorium can carry 2000 spectators at most. As the figure shows, the auditorium revolves with 132 steel wheels along four circular single tracks of steel rails. Concrete foundations provide vertical supports to the steel RS via the direct contact between steel rails and steel wheels. While the auditorium revolves, audience can see different scenes in a 360-degree surrounding landscape stage.

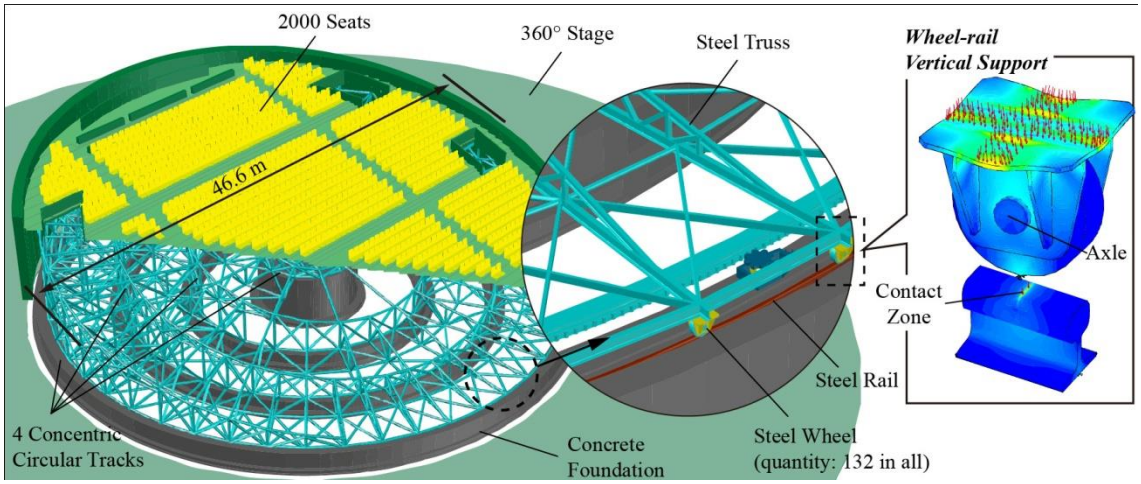

Fig. 12 Size, structure and motion of the revolving auditorium

As previously stated in Sections 2.2 and 2.3, it is necessary to consider the wheel-rail problem and to keep internal forces within a safe range during the RS revolving. For a large RS with so many wheel-rail supports, it is hard to enumerate all possible irregularity situations for all wheel-rail contacts. In the design procedure of the auditorium, a simplified method to solve the wheel-rail problem is adopted. For each structural member to consider, Member a, a sensitive local region around it, Γ_a, is defined roughly. Then all m possibilities of wheel-rail contact situations in

this region are enumerated. Finally, for each load case, all corresponding internal force values of the structural member, σ_1, σ_2, …, σ_m, are calculated by Eq. (1). Then, the design criterion is to make sure all these values satisfy the required condition such as material strength or other allowable stress, $[\sigma]$. That is, if Γ_a contains j wheels, the condition can be expressed as

$$\sigma_1, \sigma_2, ..., \sigma_m < [\sigma] \left(m = 2^j\right) \tag{9}$$

Thus, the safety margin of RS is supposed to be increased by strengthening some corresponding structural members. To define a local region, Γ_a, in the design procedure of the auditorium, both radial irregularity and circumferential irregularity of the rail are considered, as shown in Fig. 13(a). Specifically, Γ_a surrounds one or two wheels on both adjacent tracks and the two wheels on both neighboring circumferential directions.

During the auditorium construction, an evident phenomenon has been detected. In detail, an elevation survey work on rails of three outside tracks is carried out in the beginning of construction, and the survey data indicates that top surfaces of rails undulate, as shown in Fig. 13 (b). Another phenomenon is that some wheels are detached from rail surfaces after the primary steel truss has been finished. As Fig. 14(b) shows, wheel-rail detachment can be observed just by naked eyes. Fig. 14(a) shows that the construction is almost completed.

4.2Fieldtest

4.2.1 Experimental setup

Based on the proposed problem, two field-testing plans are made. One is executed by work crews in the field after the construction is completed, and the other one is performed remotely via the Internet during official performances. Fig. 15 is the arrangement diagram of VWSs. Sensor items are named according to their measuring objects and positions, as stated on the right of the figure. The nine underlined items represent the nine VWSs installed on RS of the auditorium for the first fieldtest. The five items with parentheses represent the five VWSs removed after the first fieldtest. The other items represent VWSs added for the second fieldtest.

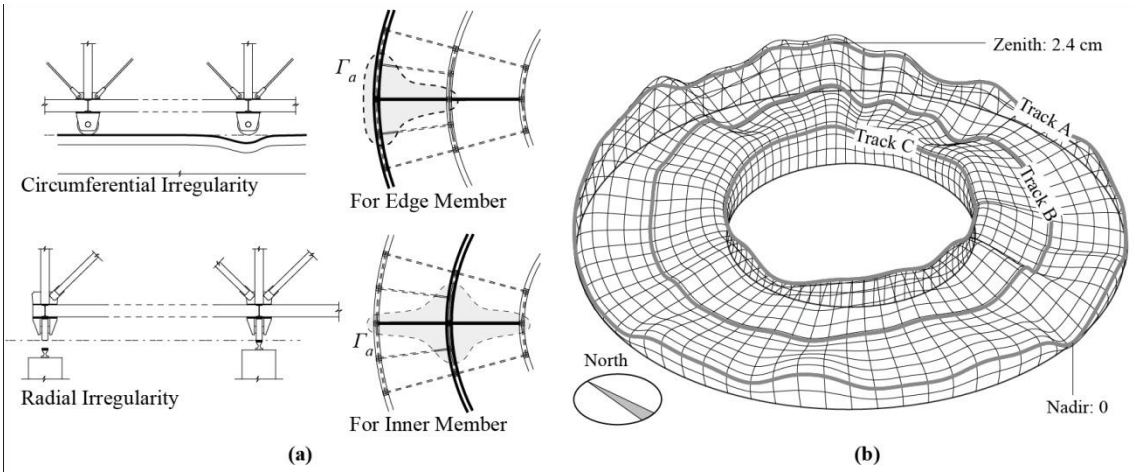

Fig. 13 Rail irregularity: (a) Local region Γ_a for irregularity consideration; (b) Elevation survey (Visual scale factor of 1: 200)

Fig. 14 (a) Photo of revolving auditorium under construction; (b) Photo of wheel-rail detachment

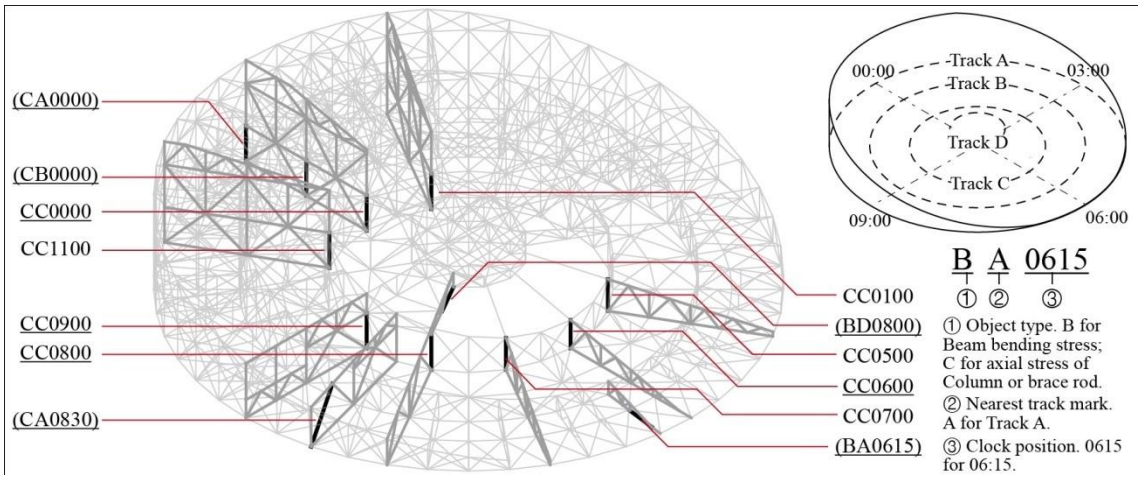

Fig. 15 Distribution of VWSs

Fig. 16 shows some installation details of the sensing system. A VWS is fixed on a structural member by two clamps welded on the member surface (Fig. 16(b)). Sensor nodes are connected with VWSs and arranged to proper positions. For example, Fig. 16(a) shows six nodes in one subnet. Fig. 16(c) shows some onsite devices of the first field test: An IPC, a two-channel sink node, two single-channel sink nodes for backup, and a laptop for onsite operations. After the first field test is completed, work crews leave the auditorium site. Then with the addition of a 3G card, those devices will be controlled remotely for the second field test.

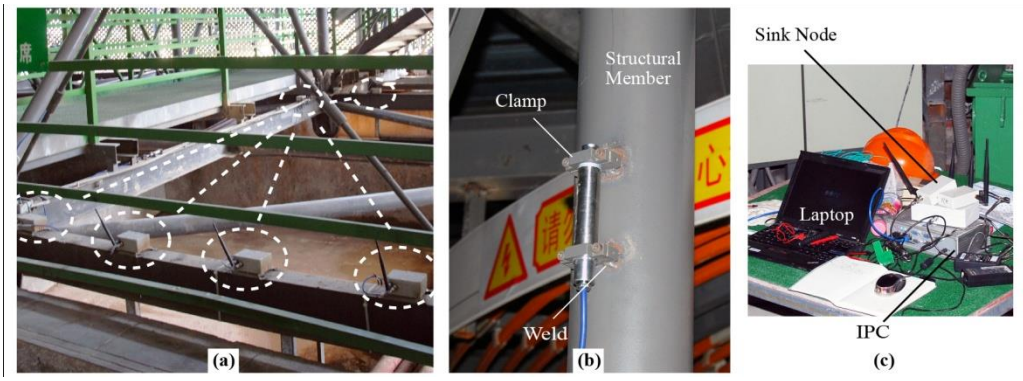

Fig. 16 Photos of system installation: (a) Several nodes in a subnet; (b) VWS installation; (c) Onsite devices

4.2.2 Field test 1: a test run carrying people

Fig. 17 shows the plan and the implementation of field test 1. The plan includes three different load cases considered in the design phase: Loading on the back-half region, loading on the entire region and loading on the front-half region. To reflect internal force characteristics during revolving under those three load cases, the plan is divided into six steps. Step ①, RS is in a state of rest, and uniform live load acts on back-half region of RS. Step ②, RS revolves with the back-half load. Step ③, RS stops, and uniform load is added on front-half region of RS. Step ④, RS revolves with the full-region load. Step ⑤, RS stops, and back-half load is removed from RS. Step ⑥, RS revolves with the front-half load.

To fulfill the plan, 2000 adults, men and women, have attended the test run. As shown at the bottom of Fig. 17, 2000 people are divided into two equal groups to simulate the back-half load and the front-half load respectively. From Step ① to Step ②, one group of 1000 people walks up to the back-half area of the auditorium, and the auditorium revolves twice (once clockwise and the other time anticlockwise).Then for Step ③ and Step ④, the other group fills the front-half area, and the auditorium revolves twice in the same way with an entire of 2000-people live load. Finally, for Step ⑤ and Step ⑥, the back-half group exits, and the auditorium revolves twice again with the front-half group.

Counting the preparatory work, the whole process went on for about 1 hour and 50 minutes. During the process, internal force data of RS was collected by the sensing system. Fig. 18 shows two photos of the test run carrying people. In photo (a), 1000 people were standing on the back-half region of the auditorium, and in photo (b), the auditorium was rotating with all 2000 people on it.

4.2.3 Field Test2: Monitoring during formal commercial operation

After the auditorium is formally in operation for *Impression Dahongpao*, some sensor nodes are added, as mentioned in Section 4.2.1. Fig. 19(a) shows a photo taken during the commercial performance. Fig. 19(b) is a rough summer schedule of the auditorium. When the auditorium is operated for performances, usually at nighttime, the status of RS of the auditorium is monitored by the sensing system, and internal force data is collected.

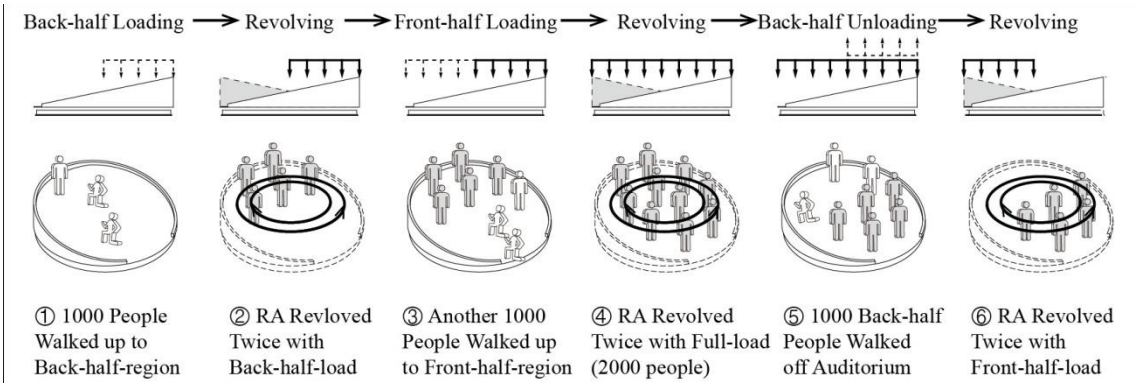

Fig. 17 Plan of test run carrying people

Fig. 18 Photos of test run carrying people: (a) 1000 people standing on the back-half region and the auditorium being ready to start; (b) Revolving with full load of 2000 people

No.	Time	Event
(1)	18:40~19:20	Routine inspection
(2)	19:30~19:55	Spectators are let in
(3)	20:00	The show starts
(4)	20:08~20:12	Keep rotating for 4min4s
(5)	20:18~20:19	Keep rotating for 1min5s
(6)	20:32~20:36	Keep rotating for 3min15s
(7)	20:51~20:56	Keep rotating for 4min57s
(8)	21:01~20:06	Keep rotating for 5min20s
(9)	21:07~20:13	Keep rotating for 5min46s
(10)	21:15	The show is over
(11)	21:15~21:30	Spectators leave
--	21:30 ...	For the next show ...

(b)

Fig. 19 Formal operation: (a) In the performance of *Impression Dahongpao*; (b) Operation schedule

5. Results and discussion

5.1 Field test 1: internal force characteristic of RS

The results of data acquisition in the test run carrying people are shown in Fig. 20. The timeline of the figure is consistent with that of Fig. 17, and the numbers in the figure, ①~⑥, correspond to Step ①~⑥ mentioned before. The figure shows time-history curves of stress values acquired from nine sensors whose corresponding structural members have been demonstrated in Fig. 15. Results of Fig. 20 manifest that the internal forces of RS fluctuate obviously while revolving. Further, it can be seen that the fluctuation extent of internal force varies from member to member, and from load case to load case. The existence and influence of the wheel-rail problem in RS, which were proposed previously, are confirmed by the field-testing results.

For these nine structural members, the design values of their internal forces are illustrated in Fig. 21, which were obtained according to Eq. (9) in the structural design process. In the figure, three load cases are respectively abbreviated as BH (Back-half), FU (Full) and FH (Front-half). It was ensured that the design values of member internal forces do not exceed the allowable range, that is to say, the fluctuation extents of internal values were estimated in the design phase.

The fluctuation extents of design values and testing values, $\Delta\sigma$ and $\Delta\sigma_t$, can be expressed as

$$\begin{aligned} \Delta\sigma &= \max\{\sigma_1, \sigma_2, ..., \sigma_m\} - \min\{\sigma_1, \sigma_2, ..., \sigma_m\}, \\ \Delta\sigma_t &= \max\{\sigma_{t,1}, \sigma_{t,2}, ..., \sigma_{t,i}\} - \min\{\sigma_{t,1}, \sigma_{t,2}, ..., \sigma_{t,i}\}. \end{aligned} \tag{10}$$

where $\sigma_{t,1}, \sigma_{t,2}, \ldots, \sigma_{t,I}$ are i data points of testing values in the relative phase. $\Delta\sigma$, according to the data of Fig. 21, and $\Delta\sigma_t$, according to the data of Fig. 20, are compared in three load cases in Table 1. It can be seen that for some members, $\Delta\sigma_t$ exceeds $\Delta\sigma$, but for most of the members, $\Delta\sigma$ covers $\Delta\sigma_t$. In other words, presumptively, if RS were designed conventionally under full-stress rule, without considering multiple possibilities of wheel-rail contacts and enhancing relative members, the structure would have failed when its internal force fluctuates during rotation. Therefore, it is important to consider the fluctuation of RS internal forces during revolving. Moreover, the effectiveness and necessity of the design procedure of Eq. (9) have been demonstrated.

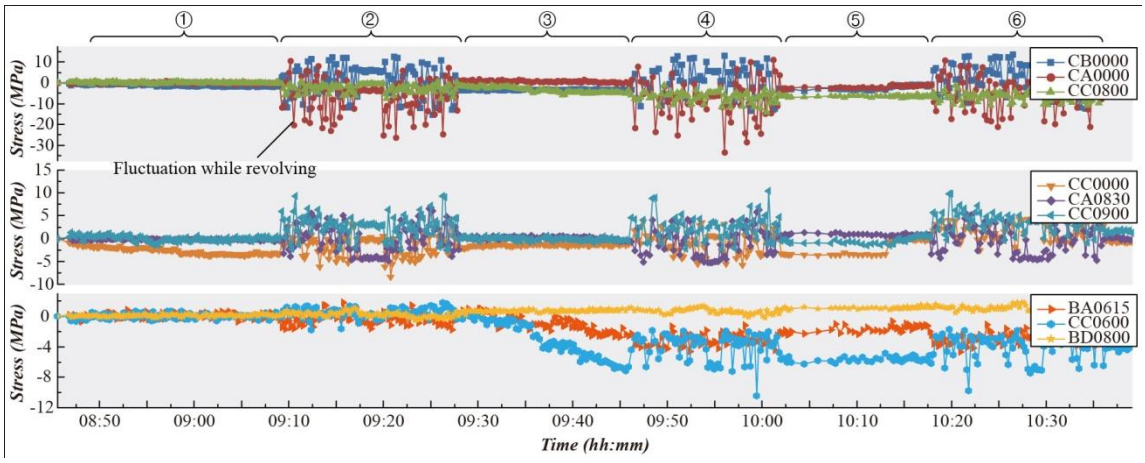

Fig. 20 The test run carrying people: Data acquisition results of the entire process

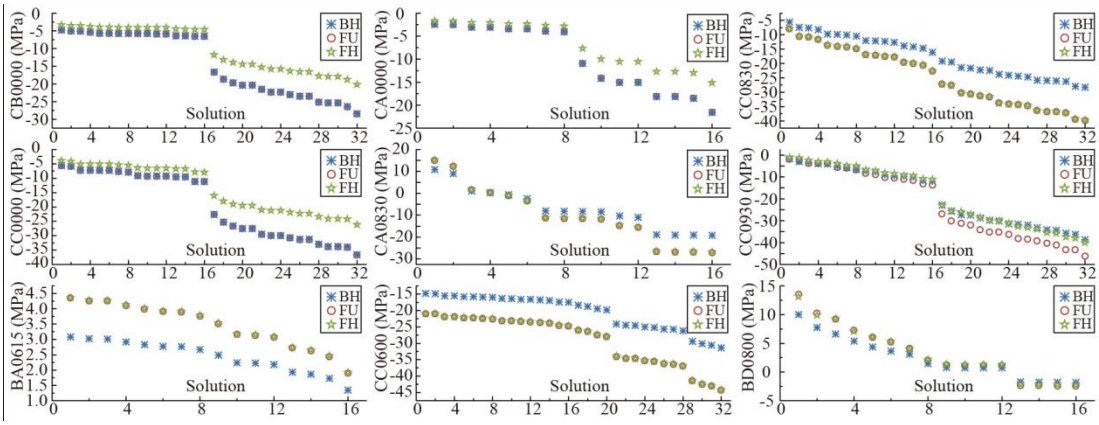

Fig. 21 Stress values in the design phase

Table 1 Fluctuation extents of design values and testing values in different load cases (MPa)

Item	$\Delta\sigma$ (design value)			$\Delta\sigma_t$ (testing value)		
	Back-half	Full	Front-half	Back-half	Full	Front-half
CB0000	23.689	23.697	16.826	28.076	26.574	26.133
CA0000	19.184	19.090	13.454	36.736	44.644	32.114
CC0800	22.668	31.866	31.815	8.539	13.006	9.491
CC0000	31.117	31.214	22.248	12.259	9.682	7.035
CA0830	30.054	42.168	42.019	11.605	11.673	10.929
CC0900	37.074	44.340	38.687	11.803	12.697	10.727
BA0615	1.739	2.449	2.448	3.584	3.955	3.945
CC0600	16.569	23.301	23.267	3.644	8.596	8.449
BD0800	11.800	15.904	15.370	1.570	1.570	1.806

5.2 Field test2: status identification

After the auditorium has been put into formal operation, the sensing system is used for health monitoring and status identification of RS. In a word, the main purpose is to inspect if the RS of the auditorium works well. For remote users who want to inspect the operation status of the auditorium from a display screen, such as technologists, administrators or officials, the data can be gathered and transmitted via the Internet. As previously mentioned, the auditorium operates following the schedule listed in Fig. 19(b). The specific operational situation of the auditorium can be verified by field-testing data. Fig. 22 shows internal force data results of an entire performance, and the status of the auditorium in time sequence is identified. The sequence numbers in the figure

are consistent with those of Fig. 19(b). With the help of the sensing system, some events can be detected, such as spectator entering and leaving, and the moment when the rotation start and ends. Even the audience number of each performance can be roughly estimated.

Another benefit of the sensing system installed on RS involves its being a source of feedback for automated and unattended control operation. Moreover, being controlled with the source of the sensing system, RS safety can be boosted in both short-term and long-term ways. On one hand, for example, the sensing system can send a signal to the control center of the revolving auditorium when there is an emergency of structural failure. Then the control center can stop power or brake the rotating structure. It is the short-term way. On the other hand, in the long-term way, after the auditorium has run for a long period, some of the structural members may suffer fatigue damage. The sensing system will help to assess the reliability of RS. The system can give advices to the control center to adjust operating parameters or strengthen the structure.

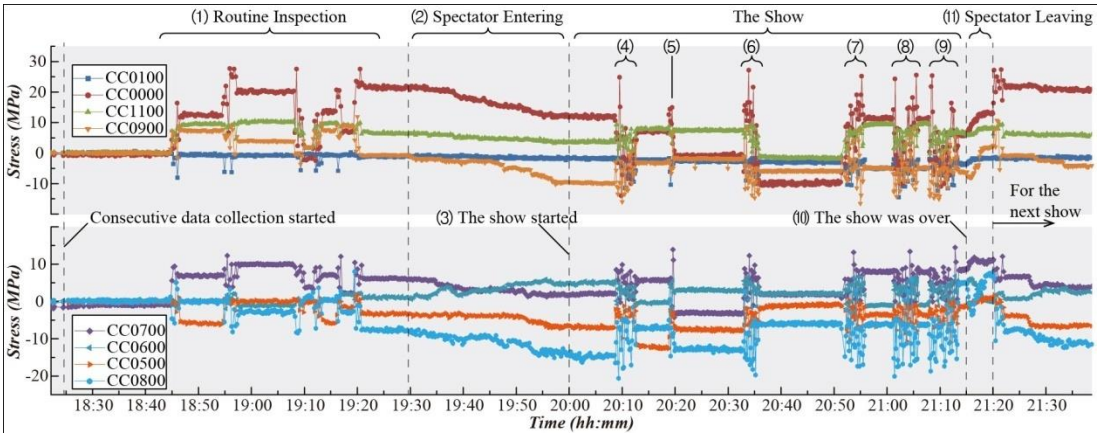

Fig. 22 Data acquisition results of a commercial performance

6. Conclusions

In this paper, a wireless dynamic sensing system is developed for RS in civil engineering. First, a wheel-rail problem of internal force redistribution during revolving caused by wheel-rail irregularity is proposed. Considering the safety of RS, the sensing system is used to collect data. The development of the system, including system architecture, network organization, sensor nodes and online remote control, is described in details. Specifically, the network organization keeps sensor network available during RS revolving. Sensor node addresses are reassigned dynamically, and network topology is reorganized accordingly. Then the sensing system is applied on a large outdoor revolving auditorium. The auditorium is designed with the consideration of the wheel-rail problem. After the auditorium is constructed, two field-testing experiments are carried out. One test involves 2000 people acting as live load for testing, and the internal force characteristics of RS during revolving in three different load cases are tested. The other test is the monitoring of the RS during its official operations, and it is executed remotely via the Internet.

According to the results from field tests, the following conclusions have been made:

●The data showed that, stress values of structural members fluctuated while RS of the

auditorium was revolving. As it is expected, the field-testing results directly verify that, the wheel-rail problem exists in RS in civil engineering, which is proposed in this paper.

●In Field Test 1, continuous data of nearly two hours were collected successfully. In Field Test 2, for every show of over three hours, data had been transmitted remotely to online terminals. It is indicated that, for RS, the sensing system developed in this paper provides a durable tool to collect structural internal force data and monitor the behavior of RS. Without doubt, for movable structures in civil engineering, especially for larger ones, wireless way and dynamic network reorganization can be very helpful for SHM.

●In the design process of the revolving auditorium in this paper, multiple internal force values of different irregularity situations were calculated. To keep all these values within the allowable range, sections of corresponding structural members were enhanced. This paper offers a solution to deal with the wheel-rail problem by increasing the safety margin of RS, compared to conventional design method. The necessity and effectiveness of the solution were proved by the field-testing results.

●In Field Test 2, when RS was in a working state, its status could be identified according to data from the sensing system. A feedback mechanism was conceived to implement the safety control of RS. The importance of the sensing system was proved once again.

Furthermore, this paper appeals for adequate attention to the wheel-rail problem in RS design and operation, or other kinetic structures. If possible, it would be best to install sensing system on every important movable building, which will help to obtain necessary information to improve structural reliability. For further research, larger and more complex movable structures would be studied. Development of sensing systems will aim more at larger scales, lower costs, lower power consumption, smarter dynamic networking and more flexible controlling.

Acknowledgments

This work was financially supported by The National Key Technology R&D Program (2012BAJ07B03) and The National Natural Science Foundation of China (Grant No.51178415).

References

Akyildiz, I.F., Su, W., Sankarasubramaniam, Y. and Cayirci, E. (2002), "Wireless sensor networks: a survey", *Computer Netw.*, **38**(4), 393-422.

Barke, D.W. and Chiu, W.K. (2005), "A review of the effects of out-of-round wheels on track and vehicle components", *Proceedings of the Institution of Mechanical Engineers, Part F: Journal of Rail and Rapid Transit*, **219**(3), 151-175.

Basheer, M.R., Rao, V. and Derriso, M. (2003), "Self organizing wireless sensor networks for structural health monitoring", *Proceedings of the SPIE - The International Society for Optical Engineering: Smart Structures and Materials 2003 Modeling, Signal Processing, and Control*, San Diego, CA, United states, March 3- March 6.

Bourland, M.C. and Yuan, R.L. (2008), *Vibrating wire strain gages and civil structures*, Earth & Space 2008, ASCE Press, Reston, VA, United States.

Bourquin, F. and Joly, M. (2005), "A magnet-based vibrating wire sensor: design and simulation", *Smart Mater. Struct.*, **14**(1), 247.

Catbas, F., Zaurin, R., Gul, M., Sardinas, A., Dumlupinar, T., Gokce, H. and Terrell, T. (2010), "Heavy

movable structure health monitoring: a case study with a movable bridge in Florida", *Proceedings of the Structures Congress 2010*, ASCE Press, Reston, VA, United States.
Coutts, D.R., Wang, J. and Cai, J.G. (2001), "Monitoring and analysis of results for two strutted deep excavations using vibrating wire strain gauges", *Tunn. Undergr. Sp. Tech.*, **16**(2), 87-92.
Dumlupinar, T., Gokce, H.B., Catbas, F.N. and Frangopol, D.M. (2011), "Time-variant reliability and load rating of a movable bridge using structural health monitoring", *Proceedings of the 28th IMAC, A Conference on Structural Dynamics, 2010*, Jacksonville, FL, United states, February 1-4.
Felegyhazi, M. (2001), *Development and evaluation of a dynamic bluetooth scatternet formation procedure, Master*, Dissertation, Budapest University of Technology and Economics, Budapest, Hungary.
Frampton, K., Galfetti, A. and Farinati, V. (2006), *Villa Girasole. La casa rotante / The Revolving House*, Mendrisio Academy Press, Mendrisio, Switzerland.
Gokce, H., Gul, M. and Catbas, F. (2012), "Implementation of structural health monitoring for movable bridges", *Transport. Res. Record*, (2313), 124-133.
Grassie, S.L., Gregory, R.W., Harrison, D. and Johnson, K.L. (1982), "The dynamic response of railway track to high frequency vertical excitation", *J. Mech. Eng. Sci.*, **24**(2), 77-90.
Kim, J.T., Nguyen, K.D. and Thanh, C. (2013), "Wireless health monitoring of stay cable using piezoelectric strain response and smart skin technique", *Smart Struct. Syst.*, **12**(3-4), 381-397.
Kim, S., Pakzad, S., Culler, D., Demmel, J., Fenves, G., Glaser, S., Turon, M. and Acm (2007), "Health monitoring of civil infrastructures using wireless sensor networks", *Proceedings of the 6th International Symposium on Information Processing in Sensor Networks*, New York.
Knothe, K.L. and Grassie, S.L. (1993), "Modelling of railway track and vehicle/track interaction at high frequencies", *Vehicle Syst. Dyn.*, **22**(3-4), 209-262.
Lee, H.M., Kim, J.M., Sho, K. and Park, H.S. (2010), "A wireless vibrating wire sensor node for continuous structural health monitoring", *Smart Mater. Struct.*, **19**(5), 055004.
Linderman, L., Rice, J., Barot, S., Spencer, B. and Bernhard, J. (2010), "Characterization of wireless smart sensor performance", *J. Eng. Mech. – ASCE*, **136**(12), 1435-1443.
Lynch, J.P., Sundararajan, A., Law, K.H., Kiremidjian, A.S., Kenny, T. and Carryer, E. (2003), "Embedment of structural monitoring algorithms in a wireless sensing unit", *Struct. Eng. Mech.*, **15**, 285-297.
Lynch, J.P., Law, K.H., Kiremidjian, A.S., Carryer, E., Farrar, C.R., Sohn, H., Allen, D.W., Nadler, B. and Wait, J.R. (2004), "Design and performance validation of a wireless sensing unit for structural monitoring applications", *Struct. Eng. Mech.*, **17**(3-4), 393-408.
Lynch, J.P., Wang, Y., Loh, K.J., Yi, J.H. and Yun, C.B. (2006), "Performance monitoring of the Geumdang Bridge using a dense network of high-resolution wireless sensors", *Smart Mater. Struct.*, **15**(6), 1561.
Myung, H., Lee, S. and Lee, B. (2011), "Paired structured light for structural health monitoring robot system", *Struct. Health Monit.*, **10**(1), 49-64.
Nagayama, T., Spencer, B.F. and Rice, J.A. (2009), "Autonomous decentralized structural health monitoring using smart sensors", *Struct. Control Health Monit.*, **16**(7-8), 842-859.
Neild, S.A., Williams, M.S. and McFadden, P.D. (2005), "Development of a vibrating wire strain gauge for measuring small strains in concrete beams", *Strain*, **41**(1), 3-9.
Ni, Y.Q., Xia, Y., Liao, W.Y. and Ko, J.M. (2009), "Technology innovation in developing the structural health monitoring system for Guangzhou New TV Tower", *Struct. Control Health Monit.*, **16**(1), 73-98.
Ramzy, N. and Fayed, H. (2011), "Kinetic systems in architecture: New approach for environmental control systems and context-sensitive buildings", *Sustain.Cities Soc.*, **1**(3), 170-177.
Randl, C. (2008), *Revolving architecture: a history of buildings that rotate, swivel, and pivot*, Princeton Architectural Press, New York.
Sato, Y. (1977), "Study on high-frequency vibrations in track operated with high-speed trains", *Railway Technical Research Institute, Quarterly Reports*, **18**(3), 109-114.
Sazonov, E., Jha, R., Janoyan, K., Krishnamurthy, V., Fuchs, M. and Cross, K. (2006), "Wireless intelligent sensor and actuator network (WISAN): a scalable ultra-low-power platform for structural health monitoring", *Proceedings of the SPIE 6177, Health Monitoring and Smart Nondestructive Evaluation of Structural and Biological Systems V*, San Diego, CA, United States, FEB 27-MAR 01, 2006, **6177**,

61770S1-61770S11.

Spencer, B.F., Ruiz-Sandoval, M.E. and Kurata, N. (2004), "Smart sensing technology: opportunities and challenges", *Struct. Control Health Monit.*, **11**(4), 349-368.

Steffens, D.M. (2005), *Identification and development of a model of railway track dynamic behaviour*, Master Dissertation, Queensland University of Technology, Brisbane, Australia.

Straser, E.G. and Kiremidjian, A.S. (1998), *A modular, wireless damage monitoring system for structures*, John A. Blume Earthquake Engineering Center, Department of Civil and Environmental Engineering, Stanford University, Report No. 129, Stanford, CA, United States.

Teng, J., Zhu, Y., Lu, W. and Xiao, Y. (2010), "The intelligent method and implementation of health monitoring system for large span structures", *Proceedings of the Earth and Space 2010*, ASCE Press, Reston, VA, United States.

Thompson, D.J. (1991), "Theoretical modelling of wheel-rail noise generation", *Proceedings of the Institution of Mechanical Engineers, Part F: Journal of Rail and Rapid Transit*, **205**(2), 137-149.

Timoshenko, S. (1926), "Method of analysis of statical and dynamical stresses in rail", *Proceedings of the 2nd International Congress for Applied Mechanics*, Zurich, Swiss.

Tomas, S.L. and Gonzalo, H.C. (2012), "A dynamic and distributed addressing and routing protocol for wireless sensor networks", *Proceedings of the 8th Annual International Conference on Mobile and Ubiquitous Systems: Computing, Networking and Services, MobiQuitous 2011*, Copenhagen, Denmark, December 6, 2011 - December 9, 2011.

Wang, Y., Lynch, J.P. and Law, K.H. (2005), "Wireless structural sensors using reliable communication protocols for data acquisition and interrogation", *Proceedings of the Society for Experimental Mechanics (SEM), 23rd Conference and Exposition on Structural Dynamics 2005, IMAC-XXIII*, Orlando, FL, United states, January 31, 2005 - February 3, 2005.

Wang, Y., Lynch, J.P. and Law, K.H. (2007), "A wireless structural health monitoring system with multithreaded sensing devices: design and validation", *Struct. Infrastruct. E.*, **3**(2), 103-120.

Wang, Y. and Law, K. (2011), "Structural control with multi-subnet wireless sensing feedback: experimental validation of time-delayed decentralized H-infinity control design", *Adv. Struct. Eng.*, **14**(1), 25-39.

Wigginton, M. and Harris, J. (2002), *Intelligent skins*, Butterworth-Heinemann, Oxford.

Yao, Z. and Dressler, F. (2007), "Dynamic address allocation for management and control in wireless sensor networks", *Proceedings of the 40th Annual Hawaii International Conference on System Sciences 2007, HICSS'07*, Big Island, HI, United states, January 3, 2007 - January 6, 2007.

Yu, F. and Gupta, N. (2005), "An efficient model for improving performance of vibrating-wire instruments", *Measurement*, **37**(3), 278-283.

Yun, C.B., Cho, S., Park, H.J., Min, J. and Park, J.W. (2013), "Smart wireless sensing and assessment for civil infrastructure", *Struct. Infrastruct. E.*, **10**(4), 534-550.

Zhu, D., Yi, X., Wang, Y., Lee, K.M. and Guo, J. (2010), "A mobile sensing system for structural health monitoring: design and validation", *Smart Mater. Struct.*, **19**(5), 055011.